Supplemental Materials for Nonclassical Nucleation in a Solid-Solid Transition of Confined Hard Spheres"

Weikai Qi,[1,2] Yi Peng,[3] Yilong Han,[3] Richard K. Bowles,[2] and Marjolein Dijkstra[1,*]

[1] *Soft Condensed Matter, Debye Institute for Nanomaterials Science, Utrecht University, Princetonplein 5, 3584 CC Utrecht, The Netherlands*

[2] *Department of Chemistry, University of Saskatchewan, Saskatoon, Saskatchewan S7N 5C9, Canada*

[3] *Department of Physics, Hong Kong University of Science and Technology, Clear Water Bay, Hong Kong, China*

(Dated: September 23, 2015)

I. PHASE BEHAVIOR OF CONFINED HARD SPHERES: THE $5\square \rightarrow 4\triangle$ TRANSITION

We consider a system consisting of N hard spheres of diameter σ confined between two parallel hard walls with a surface area A and separated by a distance $H/\sigma = 4$. The packing fraction for the system is defined as $\eta = \pi N\sigma^3/(6AH)$. According to free-energy calculations [1], the system exhibits a first-order phase transition from a liquid to a crystal phase consisting of four triangular layers ($4\triangle$), and a first-order phase transition from the $4\triangle$ crystal phase to a crystal phase consisting of five square layers ($5\square$) with a $5\square - 4\triangle$ phase coexisting regime $0.537 < \eta < 0.571$.

To obtain the chemical potential differences between the phases in the metastable regions of the phase diagram, we use event-driven molecular dynamics (EDMD) simulations to calculate the equation of state. In an EDMD simulation, the system evolves via a time-ordered sequence of elastic collision events, which are described by Newton's equations of motion. The spheres move at constant velocity between collisions, and their velocities are updated when a collision occurs. We compute the reduced 2D lateral pressure $P^* = \beta P\sigma^2$ via the virial theorem,

$$P^* = \beta P\sigma^2 = \frac{N\sigma^2}{A}\left[1 - \frac{\beta m}{2t}\frac{1}{N}\sum_{i<j}^{N}\mathbf{r}_{ij}\cdot\mathbf{v}_{ij}\right], \qquad (1)$$

where $m = 1$ is the mass of the particles, $N = 12500$ is the number of particles, $\beta = 1/k_BT$, k_B is the Boltzmann constant, T is the temperature, $\mathbf{r}_{ij}$ and $\mathbf{v}_{ij}$ are respectively the displacement and velocity of particle i relative to those of particle j, and t is the time interval. Time is measured in MD units $\tau = \sqrt{\frac{m\sigma^2}{k_BT}}$. The system is equilibrated for 800τ, and the pressure is measured for an additional 200τ. Figure S1 shows the equations of states obtained from the simulation.

In this work, we study the kinetics of the phase transition from a metastable $5\square$-crystal to a stable $4\triangle$-crystal phase. A phase diagram in the literature shows that for $\eta < 0.571$, the $4\triangle$-crystal phase is thermodynamically stable as its free energy is lower than that of the $5\square$ phase [1]. Using the $5\square$-crystal phase as the initial configuration in our simulations, we find that this phase remains metastable down to a pressure $P^* = 35.8$, which corresponds to a packing fraction $\eta = 0.479$. We also note that at $\eta = 0.479$, both the $4\triangle$ and $5\square$ crystals have the same pressure $P^* = 35.8$. The $5\square$-crystal phase is thus metastable in the region $0.479 < \eta < 0.571$. Due to the limited simulation time, a critical nucleus cannot form in the $5\square \rightarrow 4\triangle$ transition at $\eta > 0.500$. We calculate the chemical potentials of each phase using thermodynamic integration along the equation of state. For $\eta \leq 0.500$, the chemical potential difference between the $5\square$-solid and liquid phases, $\mu_{\square-L}$, decreases with increasing packing fraction η (see Table 1 or Fig. S2). This reduces the thermodynamic driving force for nucleation and lowers the probability of observing liquid droplets through density fluctuations in our simulations. As a result, we

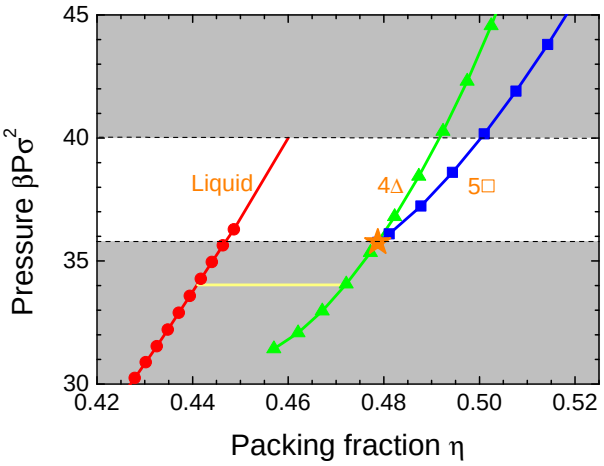

FIG. S1. Equations of states (i.e. the reduced 2D lateral pressure $P^* = \beta P\sigma^2$ as a function of packing fraction η) of the liquid (dots), $4\triangle$ crystal (triangles) and $5\square$ crystal (squares) phases in a system of hard spheres confined between two planar hard walls separated by a distance $H/\sigma = 4$. Curves are the fifth degree polynomial fittings of equations of states of the liquid (red), $4\triangle$ crystal (green) and $5\square$ crystal (blue) phases. The yellow line indicates the region where the liquid and $4\triangle$ crystal phases coexist and the star indicates the point where the pressure is the same for both the $4\triangle$ and $5\square$ crystal phases. Our nucleation study is carried out in the region $35.8 \leq P^* \leq 40$ (white area between the dotted lines).

* M.Dijkstra1@uu.nl

P^*	η_L	$\eta_\triangle$	$\eta_\square$	$\beta\mu_L$	$\beta\mu_\triangle$	$\beta\mu_\square$	$\beta\mu_{\square-L}$	$\beta\mu_{L-\triangle}$
40	0.460	0.492	0.500	15.14	15.02	15.34	0.20	0.12
39	0.457	0.489	0.496	14.85	14.75	15.08	0.23	0.10
38	0.454	0.486	0.491	14.56	14.48	14.81	0.25	0.08
37	0.451	0.483	0.487	14.27	14.21	14.54	0.27	0.06

TABLE I. Pressure $P^* = \beta P\sigma^2$, packing fraction η and chemical potentials $\beta\mu$ for the liquid, 4△-solid and 5□-solid phases. $\beta\mu_{\square-L}$ is the chemical potential difference between 5□ and the liquid, and $\beta\mu_{L-\triangle}$ is the chemical potential difference between the liquid and the 4△-solid phase.

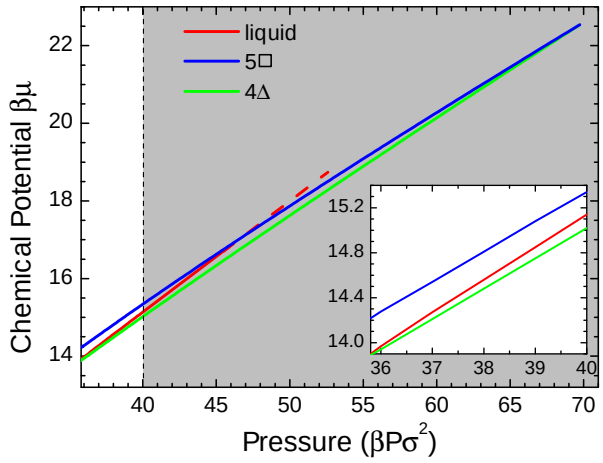

FIG. S2. Chemical potentials $\beta\mu$ for the liquid, 4△ and 5□ phases in the region $35.8 < P^* < 70$ where the liquid and 5□ are metastable. Inset shows chemical potentials in the region $35.8 \leq P^* \leq 40$.

focus on nucleation in the region $0.479 \leq \eta \leq 0.500$ or $35.8 \leq P^* \leq 40$.

II. FORMATION OF A LIQUID DROPLET IN THE SOLID-SOLID TRANSITION

In the EDMD simulations, the defect-free 5□-solid phase at packing fraction $\eta = 0.490$ developed small liquid-like clusters which fluctuated in size. After a long induction time, a critical liquid nucleus appeared embedding a 4△-nucleus. The bond orientational order parameter Ψ_6 has been used to distinguish among the fluid-, 4△-, and 5□-like particles in the main text. However, as the liquid-like particles move much faster than the crystalline particles, one can also employ a dynamic criterion. To this end, we measure the self-part of the Van Hove correlation function as defined by [2]

$$G_s(R,t) = \frac{1}{N}\left\langle \sum_i^N \delta\left(R - |\mathbf{R}_i(t+t_w) - \mathbf{R}_i(t_w)|\right)\right\rangle, \quad (2)$$

where $\mathbf{R}_i(t)$ is the position of particle i at time t, and R the diffusion distance of the particles during time interval t. At short waiting times, the Van Hove correlation function is Gaussian. As soon as a liquid nucleus starts to

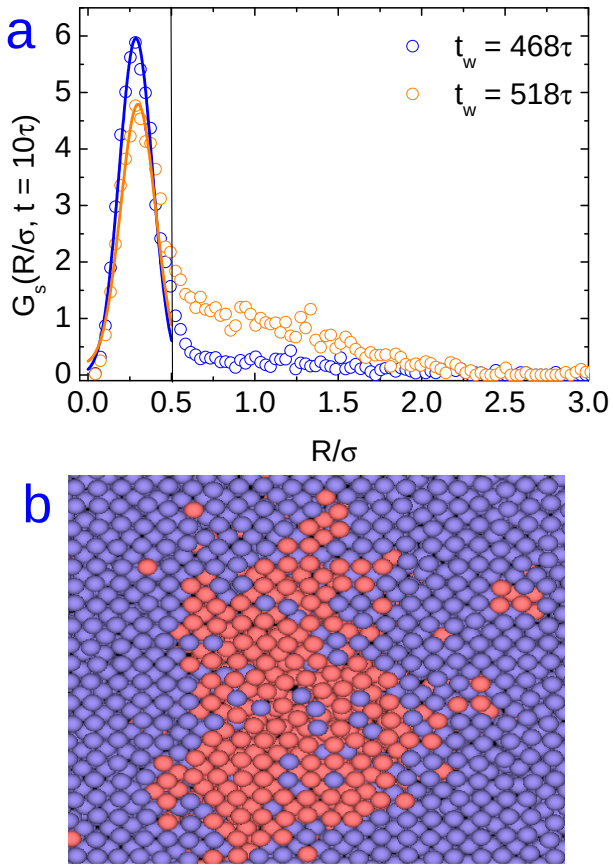

FIG. S3. (a) Self-part of the Van Hove correlation function $G(R, t = 10\tau)$ at waiting times $t_w = 468\tau$ and $t_w = 518\tau$. The vertical line marks the non-Gaussian long tails corresponding to the fast-moving particles. Solid curves are the Gaussian fits. (b) A typical configuration at waiting time $t_w = 518\tau$ of the EDMD simulation at packing fraction $\eta = 0.490$. The red and blue particles denote the fast-moving and slow-moving particles, respectively.

grow at waiting times $t_w = 468\tau$ and 518τ, the Van Hove correlation function becomes non-Gaussian as shown in Fig. S3a. The long tail of the self-part of the Van Hove correlation function indicates the presence of liquid-like particles with higher mobilities than the solid-like particles. In Fig. S3b, the fast-moving particles, i.e. those with displacement $> 0.5\sigma$ in a time interval $t = 10\tau$, correspond to disordered fluid-like particles, which confirms

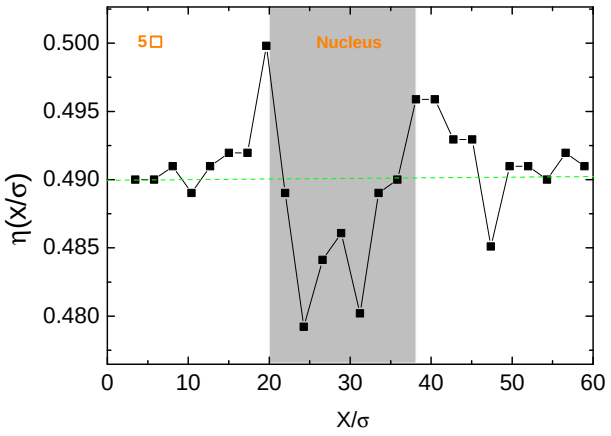

FIG. S4. The density profile across the diameter of the cluster at waiting time $t_w = 518\tau$ in MD time units and at a packing fraction $\eta = 0.490$. The green dashed line denotes the packing fraction of the metastable 5□ phase. The location of the liquid-4△ nucleus is denoted by the shaded region.

the formation of a liquid-like droplet in the nucleation process. In addition, the density profile of the cluster in Fig. S4 confirms the formation of a liquid-like droplet. The packing fraction a long way from the nucleus approaches that of the metastable 5□ phase.

III. CLASSICAL NUCLEATION THEORY FOR THE $5\square \rightarrow 4\triangle$ SOLID-SOLID TRANSITION

We consider a simple model for the nucleation process. We assume that nucleation proceeds via the formation of a nucleus consisting of liquid-like and △-solid-like particles. In addition, we assume that the nucleus is cylindrical with height H and consists of a cylindrical core of △-solid-like particles surrounded by a cylindrical ring of liquid. We first consider two systems as shown in Fig. S5. System I contains the homogeneous metastable 5□ phase, characterized by entropy S^I, volume V^I, and number of particles N, confined between two planar hard walls of total area $A_{tot} = 2A$, where A is the surface area of a single wall. System II contains a cluster consisting of N_L liquid particles and $N_\triangle$ particles of the 4△−solid phase.

The difference between the Gibbs free energies of systems II and I is then given by

$$\begin{aligned}\Delta G = &(\mu_L - \mu_\square)N_L + (\mu_\triangle - \mu_\square)N_\triangle \\ &+(\gamma_{\triangle W} - \gamma_{\square W})A_\triangle + (\gamma_{LW} - \gamma_{\square W})A_L \\ &+\gamma_{\triangle L}A_{\triangle L} + \gamma_{L\square}A_{L\square},\end{aligned} \tag{3}$$

where $\gamma_{\alpha\beta}$ and $A_{\alpha\beta}$ are the surface free energy (tension) and surface area for the $\alpha - \beta$ interface respectively, where α, β refer to $L, \square, \triangle$ and the hard wall, W. For a cylindrical core of △-solid-like particles surrounded by a cylindrical ring of liquid-like particles, we have $A_\triangle = 2N_\triangle/(H\rho_\triangle)$, $A_L = 2N_L/(H\rho_L)$, $A_{\triangle L} = \sqrt{4\pi H/\rho_\triangle}\sqrt{N_\triangle}$ and $A_{L\square} = \sqrt{4\pi H/\rho_L}\sqrt{(\rho_L/\rho_\triangle)N_\triangle + N_L}$. The Gibbs free-energy difference then reads

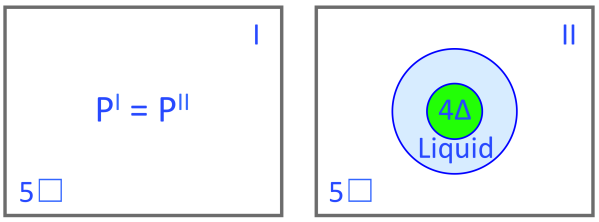

FIG. S5. A simple model for nucleation in a solid-solid transition. System I contains the homogeneous metastable 5□-solid phase confined between two planar hard walls. System II contains a cluster consisting of a 4△−solid-like core, surrounded by a liquid-like nucleus in a 5□ solid confined between the same two walls.

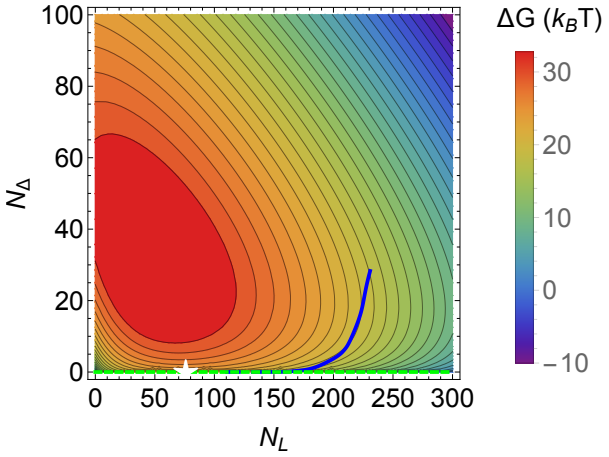

FIG. S6. Contour Plot of $\beta\Delta G(N_L, N_\triangle)$ as obtained from classical nucleation theory for the $5\square \rightarrow 4\triangle$ solid-solid transition at pressure $P^* = 40$. The green line represents a transition pathway along the $N_\square$ axis at $N_L = 0$, and the blue line represents a transition pathway along a contour line of the surface.

$$\begin{aligned}\Delta G = &\left[\mu_L - \mu_\square + \frac{2}{H\rho_L}(\gamma_{LW} - \gamma_{\square W})\right]N_L \\ &+\left[\mu_\triangle - \mu_\square + \frac{2}{H\rho_\triangle}(\gamma_{\triangle W} - \gamma_{\square W})\right]N_\triangle \\ &+\gamma_{\triangle L}\sqrt{\frac{4\pi H N_\triangle}{\rho_\triangle}} \\ &+\gamma_{L\square}\sqrt{\frac{4\pi H}{\rho_L}\left(\frac{\rho_L}{\rho_\triangle}N_\triangle + N_L\right)}.\end{aligned} \tag{4}$$

Figure S6 shows the free-energy landscape $\Delta G(N_L, N_\triangle)$ obtained from Eq. 4 at pressure $P^* = 40$, where we have used the wall-fluid interfacial tension $\beta\gamma_{LW}\sigma^2 = 1.990$, the wall-△ solid interfacial tension $\beta\gamma_{\triangle W}\sigma^2 = 1.457$, the wall-□ solid interfacial tension $\beta\gamma_{\square W}\sigma^2 = 2.106$ [1], and the liquid-solid interfacial

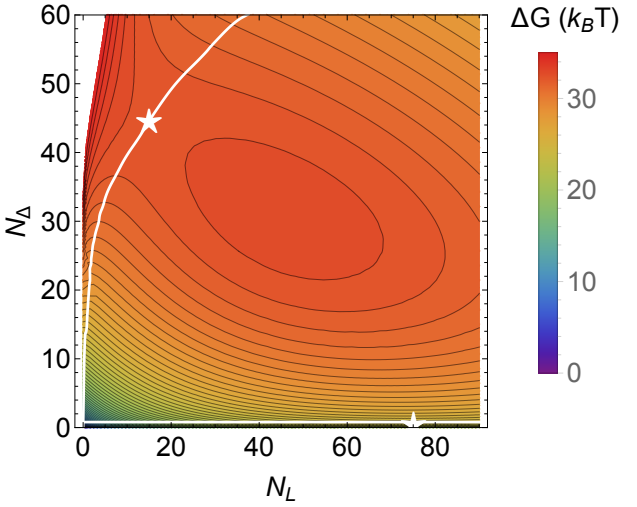

FIG. S7. Contour Plot of $\beta\Delta G(N_L, N_\triangle)$ as obtained from the modified CNT model for the $5\square \rightarrow 4\triangle$ solid-solid transition at pressure $P^* = 40$ with parameters $S = 0.03$, $\xi = 0.5$ and $\delta\epsilon = 0$. The saddle points are marked by stars. White lines represent transition pathways along the valley floor and through the saddle points.

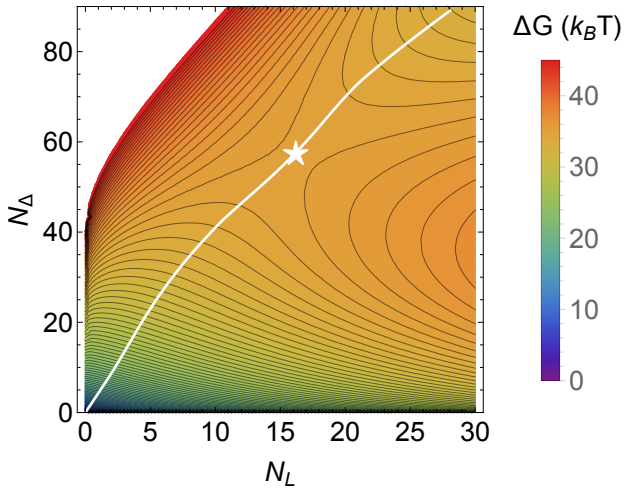

FIG. S8. Contour plot of $\beta\Delta G(N_L, N_\triangle)$ as obtained from the modified CNT model for the $5\square \rightarrow 4\triangle$ solid-solid transition at pressure $P^* = 40$ with parameters $S = 0.03$, $\xi = 0.5$ and $\delta\epsilon = 0.15$. The saddle points are marked by stars. The white line represents transition pathways along the valley floor and through the saddle point.

tension $\beta\gamma_{LT}\sigma^2 = 0.62$ and $\beta\gamma_{L\square}\sigma^2 = 0.62$ [3]. The free-energy surface shows that a high free-energy barrier stands between the $5\square$-solid and the $4\triangle$-solid phase (i.e. a path along the $N_\square$ axis at $N_L = 0$) due to the large free-energy cost associated with the formation of an interface between the two solid phases. This prevents a direct transformation of the $5\square-$solid to the $4\triangle-$solid phase. Instead, a lower free-energy path involves the formation of a liquid droplet, which beyond the saddle point grows spontaneously into the metastable liquid. The free-energy basin associated with the $4\triangle$-solid phase is separated from the liquid basin by a ridge on the free-energy surface. This free-energy surface is representative of a two-step nucleation mechanism where a liquid droplet first forms and grows before the solid phase nucleates, yielding two separate free-energy barriers. However, it is also interesting to note that clusters of the $4\triangle$-crystal can grow inside a critical liquid-like cluster without incurring an additional free-energy cost by following a path along the contour lines of the surface. The free energy surface obtained here differs from the one obtained in our free-energy calculations in Monte Carlo simulations using umbrella sampling.

IV. MODIFIED CNT MODEL

Now we consider two corrections of the classical nucleation theorem (CNT) model. The first correction term accounts for the disjoining pressure between the $5\square$-liquid and liquid-$4\triangle$ interfaces [4, 5]

$$\Delta G_{\square-liquid-\triangle} = A_{\square L} S \exp\left[-(r_L - r_\square)/\xi\right], \qquad (5)$$

where $S = \gamma_{\square\triangle} - \gamma_{\triangle L} - \gamma_{L\square}$ is the spreading parameter, r is the nucleus radius, and ξ is the range of interaction between the two interfaces. For $S = 0$, the contribution of the disjoining pressure is zero. The second correction term is the strain energy $E_{strain} \simeq N_L\Delta\epsilon$ associated with the expansion of the nucleus [6]. By adding the two correction terms to the CNT model, the free energy of formation of a nucleus is then given by

$$\begin{aligned}\Delta G = &\left[\mu_L - \mu_\square + \Delta\epsilon + \frac{2}{H\rho_L}(\gamma_{LW} - \gamma_{\square W})\right] N_L \\ &+ \left[\mu_\triangle - \mu_\square + \frac{2}{H\rho_\triangle}(\gamma_{\triangle W} - \gamma_{\square W})\right] N_\triangle \\ &+\gamma_{\triangle L}\sqrt{\frac{4\pi H N_\triangle}{\rho_\triangle}} \\ &+\gamma_{L\square}\sqrt{\frac{4\pi H}{\rho_L}\left(\frac{\rho_L}{\rho_\triangle}N_\triangle + N_L\right)} \\ &+S\exp\left[-(r_L - r_\square)/\xi\right]\sqrt{\frac{4\pi H}{\rho_L}\left(\frac{\rho_L}{\rho_\triangle}N_\triangle + N_L\right)}\end{aligned} \qquad (6)$$

As the values of $\gamma_{\square\triangle}$, ξ and $\Delta\epsilon$ are unknown, we treat them as free parameters in the modified CNT model. We set $\xi = 0.5\sigma$ and find that the value of ξ does not affect the shape of the free-energy surface. Figure S7 is the free-energy surface of the modified CNT model with parameters $\beta S\sigma^2 = 0.03$ and $\Delta\epsilon = 0$. There are two saddle points as denoted by the white asterisks in Figure S7, one for the pure liquid nucleus and the other for the liquid-$\triangle$ nucleus. As the value of the spreading parameter S increases, the saddle point of the liquid-$\triangle$

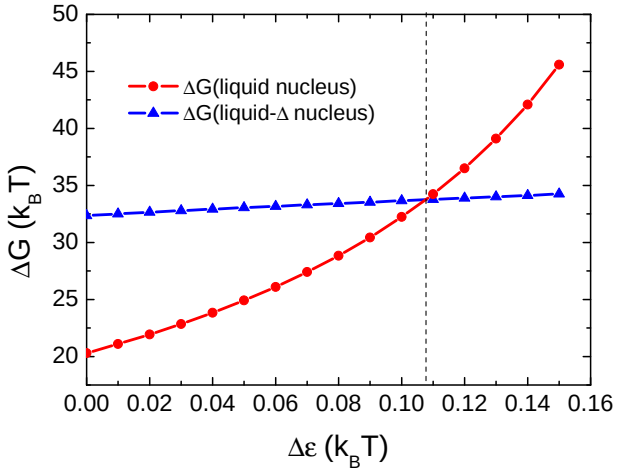

FIG. S9. The free energy barriers of the pure liquid nucleus and liquid-△ nucleus as a function of strain energy $\Delta\epsilon$ at $P^* = 40$. The other parameters are $\beta S\sigma^2 = 0.03$ and $\xi = 0.5\sigma$.

nucleus moves towards the saddle point of the pure liquid nucleus, but the lowest free-energy pathway is always the one along the saddle point of the pure liquid involving the formation of a liquid nucleus.

Figure S8 is the free-energy surface of the modified CNT model with parameters $S = 0.03$ and $\beta\Delta\epsilon = 0.15$, and thus includes a correction made to the strain energy of the 5□ crystal lattice. In this case, the free-energy barrier is $\Delta G = 45.6k_BT$ for the pure liquid nucleus and $\Delta G = 34.3k_BT$ for the liquid-△ nucleus. Thus, the pathway along the liquid-△ nucleus has the lowest free-energy barrier. Figure S9 shows the free-energy barriers of the pure liquid nucleus and of the liquid-△ nucleus as a function of $\Delta\epsilon$. For $\beta\Delta\epsilon < 0.108$, the nucleation process is □ → liquid → △; for $\beta\Delta\epsilon > 0.108$, the nucleation process is □ → (liquid-△) → △. Note that the modified CNT model includes the possibility of liquid-△ critical nucleus, the fluctuations leading to the growth of the critical cluster along the $N_\triangle$ axis. But in our simulation, a pure liquid nucleus is formed at the first stage of the nucleation, unlike in the simulations.

V. NUCLEATION RATES FROM EDMD SIMULATIONS

For packing fraction $\eta < 0.490$, EDMD simulations can reveal every step of the nucleation process. The nucleation rate can be calculated by employing a combination of EDMD simulations and the mean first passage time analysis [7, 8]. At each packing fraction $\eta = 0.480, 0.485, 0.488$ and 0.490, we collect 3000 nucleation trajectories and calculate the mean first passage time, $\tau(N_L)$, for the formation of the cluster containing N_L liquid particles and the mean first passage time, $\tau(N_\triangle)$, for the formation of the cluster containing $N_\triangle$ △-solid particles. These quantities are calculated independently, even though the triangular solid phase forms only in the presence of the liquid droplet. We estimate the size of the critical nucleus and the nucleation rate J by substituting the mean first passage times into the following expression [7, 8]:

$$\tau(N_i) = \frac{1}{2JV}\{1 + \mathrm{erf}[C(N_i - N_{cri})]\}, \qquad (7)$$

where $i = L, \triangle$, N_{cri} is the critical size of the nucleus, J is the nucleation rate, V is the system volume, $\mathrm{erf}(x)$ is the error function, and C represents the curvature at the top of the nucleation barrier. Figure S10 shows the mean first passage times at $\eta = 0.480, 0.485, and 0.488$. The corresponding fitting parameters of Eq.(7) are presented in Table II. The critical size of the 4△ nucleus does not change appreciably across η. In addition, we find that the nucleation rates J for the liquid-like and 4△ solid-like clusters are very similar, which suggests that they describe the same nucleation barrier. The difference between the nucleation rates increases only slightly with decreasing η, which indicates that the △-solid nucleates within a liquid nucleus.

[1] A. Fortini and M. Dijkstra, J. Phys.: Condens. Matter **18**, L371 (2006).
[2] K. Zahn and G. Maret, Phys. Rev. Lett. **85**, 3656 (2000).
[3] A. Härtel, M. Oettel, R. E. Rozas, S. U. Egelhaaf, J. Horbach, and H. Löwen, Phys. Rev. Lett. **108**, 226101 (2012).
[4] Y. S. Djikaev, R. Bowles, H. Reiss, K. Hämeri, A. Laaksonen, and M. Väkevä, J. Phys. Chem. B **105**, 7708 (2001).
[5] M. Iwamatsu, J. Chem. Phys. **134**, 164508 (2011).
[6] D. A. Porter, K. E. Easterling, and M. Y. Sherif, *Phase Transformations in Metals and Alloys* (CRC Press, Boca Raton, 2002).
[7] J. Wedekind, R. Strey, and D. Reguera, J. Chem. Phys. **126**, 134103 (2007).
[8] S. E. M. Lundrigan and I. Saika-Voivod, J. Chem. Phys. **131**, 104503 (2009).

	liquid			4△		
η	$J_L(\tau/\sigma^3)$	C_L	$N_{cri,L}$	$J_\triangle(\tau/\sigma^3)$	$C_\triangle$	$N_{cri,\triangle}$
0.480	3.53×10^{-6}	0.0437	395	4.07×10^{-6}	0.246	5
0.485	8.98×10^{-7}	0.0982	242	9.90×10^{-7}	0.314	6
0.488	2.40×10^{-7}	0.0157	199	2.42×10^{-7}	0.319	6
0.490	1.43×10^{-7}	0.0216	166	1.43×10^{-7}	0.394	6

TABLE II. Fitting parameters of the mean first passage time for the liquid and the 4△ solid at packing fractions $\eta = 0.480$, 0.485, 0.488 and 0.490. N_{cri} is the critical nucleus size. J_L and $J_\triangle$ are the nucleation rate for the liquid and the 4△ solid, respectively. C_L and $C_\triangle$ denote the curvature at the top of the nucleation barrier.

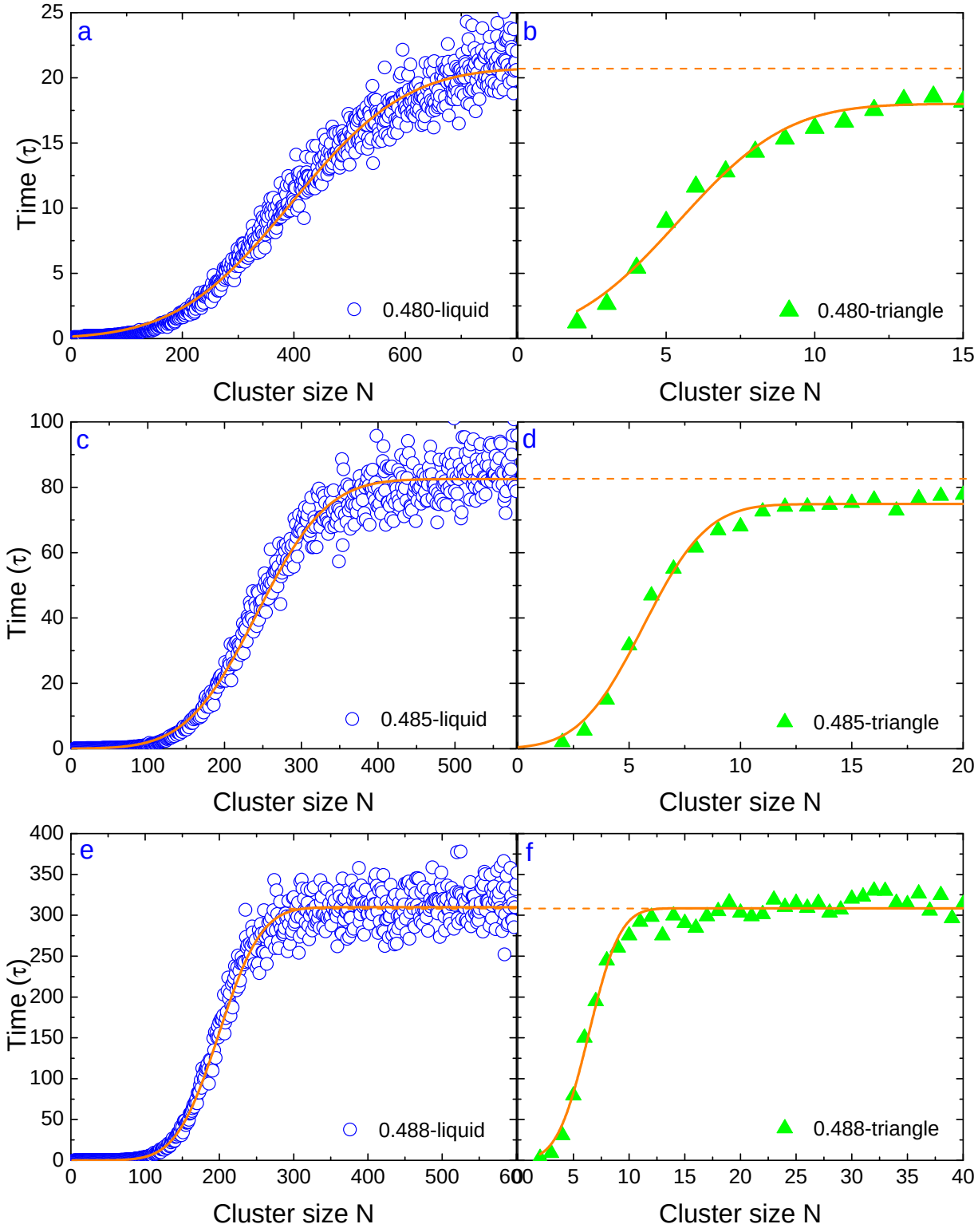

FIG. S10. The mean first passage time measured in EDMD time units for liquid-like (a, c, e) and 4△−solid-like (b, d, f) clusters as obtained from EDMD simulation at packing fractions $\eta = 0.480$ (a, b), 0.485 (c, d) and 0.488 (e, f). Lines are fits of the mean first passage time using $\frac{1}{2JV}\{1 + \mathrm{erf}[C(N - N_{cri})]\}$. The fitting parameters are shown in Table II.